Semiconductor Surfaces

International Edition: DOI: 10.1002/anie.201508828
German Edition: DOI: 10.1002/ange.201508828

Air Passivation of Chalcogen Vacancies in Two-Dimensional Semiconductors

Yuanyue Liu, Pauls Stradins, and Su-Huai Wei**

Abstract: *Defects play important roles in semiconductors (SCs). Unlike those in bulk SCs, defects in two-dimensional (2D) SCs are exposed to the surrounding environment, which can potentially modify their properties/functions. Air is a common environment, yet its impact on the defects in 2D SCs still remains elusive. Here we study the interaction between air and chalcogen vacancies (V_X), the most typical defects in 2D SCs. Although the interaction is weak for most molecules in air, O_2 can be chemisorbed at V_X with a barrier that correlates with the SC cohesive energy and can be overcome even at room temperature for certain SCs. Importantly, the chemisorbed O_2 changes the V_X from commonly believed harmful carrier-traps to electronically benign sites. This unusual behavior originates from the isovalence between O_2 and X when bonded with metal. Based on these findings, a facile approach is proposed to improve the performance of 2D SCs by using air/O_2 to passivate the defects.*

Two-dimensional (2D) semiconductors (SCs) are promising candidates for next-generation electronics, optoelectronics, and energy conversion/storage devices.[1] They feature an extremely high surface-to-mass ratio owing to their thickness of only one or several atomic layers. As a result, the atoms (including the atomic defects) are exposed to the environment that surrounds the SC, and are subjective to the environmental factors.[2] This has been demonstrated in many experiments, which show that the environment can modify the properties and performance of 2D SCs.[3]

Defects are usually more reactive than the perfect sites and therefore ought to have a stronger coupling with the environment. As defects play important roles in the properties and performance of materials, it is necessary to evaluate the impact of environment on the defects. Air is a common environment that is involved in material processing and device operation. However, its impact still remains elusive. Specifically, it is poorly understood: what is the strength of the interaction (physical or chemical), what is the effect on the electronic properties, and what is the origin of this effect?

[*] Dr. Y. Liu, Dr. P. Stradins, Dr. S.-H. Wei[+]
National Renewable Energy Laboratory
Golden, CO (USA)
E-mail: yuanyue.liu.microman@gmail.com
suhuaiwei@csrc.ac.cn
[+] Present address: Beijing Computational Science Research Center
Beijing (China)

Supporting information and ORCID(s) from the author(s) for this article are available on the WWW under http://dx.doi.org/10.1002/anie.201508828.

Chalcogen vacancies (V_X; X = S, Se, Te) are the most typical defects in 2D SCs.[4] Therefore, in this work, we investigate the interaction between air and V_X. We find that, in contrast to other molecules, O_2 can be chemisorbed at V_X. This chemisorption occurs with a barrier, which correlates with the cohesive energy of the SC and can be overcame even at room temperature for certain SCs. Importantly, the chemisorbed O_2 changes the V_X from commonly believed harmful carrier-traps to electronically benign sites. The electronic origin is explained and an effective way to improve the performance of 2D SCs is proposed.

We focus on two types of the most popular 2D SCs, namely transition-metal dichalcogenides (MX_2; M = Mo and W), and Group 13 monochalcogenides (EX, where E = Ga and In), which, in the perfect form, have good air stability at room temperature. Both types have a hexagonal unit cell with metal layers located in between two X layers. In contrast to MX_2, EX have two metal layers that form E–E bonds. First-principles calculations are performed by using the Vienna ab-initio simulation package (VASP)[5] with projector augmented wave (PAW) pseudopotentials.[6] Unless specified, the Perdew–Burke–Ernzerhof (PBE) exchange-correlation functional[7] is employed. The Heyd–Scuseria–Ernzerhof (HSE) functional (which gives a more accurate approximation of the exchange-correlation energy, but is more computationally expensive)[8] and van der Waals corrections (DFT-D3)[9] are also used in some cases to validate the robustness of the conclusions. A supercell consisting of 6×6 primitive cells is used, and the vacuum along the surface normal direction is kept to be >15 Å. The plane-wave cut-off energy is 400 eV. All the structures are relaxed until the final force on each atom is <0.01 eV Å^{-1}. The reaction barriers are calculated by using the climbing-image nudged elastic band (CINEB) method.[10]

Figure 1 shows the adsorption energies of the major molecules in air on V_x of GaS and MoS_2. The adsorption energy is defined as:

$$E_{ad} = E(V_X + mol) - E(V_X) - E(mol) \quad (1)$$

where $E(V_X + mol)$ is the energy of the system with a molecule adsorbed on the V_X site, and $E(V_X)$ and $E(mol)$ are the energies for isolated systems. Most molecules (including H_2O) are only physisorbed, that is, they are located above the top X layer with a distance of more than 2 Å (see Figure 1 inset) and adsorption energies of less than 0.2 eV. In contrast, O_2 can also be chemisorbed at V_X (see structures in Figure 2), reducing the energy by more than 1.5 eV. Adding van der Waals (vdW) corrections to the calculations shows a decrease of physisorption energies, but does not change the preference of adsorption states.

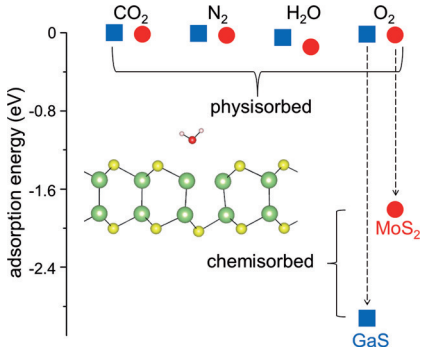

Figure 1. Adsorption energies of major molecules in air on V_X for GaS and MoS_2. Inset: the structure of H_2O adsorbed at V_X of GaS. S yellow, Ga green, O red, H white. O_2 has two adsorption states: physisorption and chemisorption.

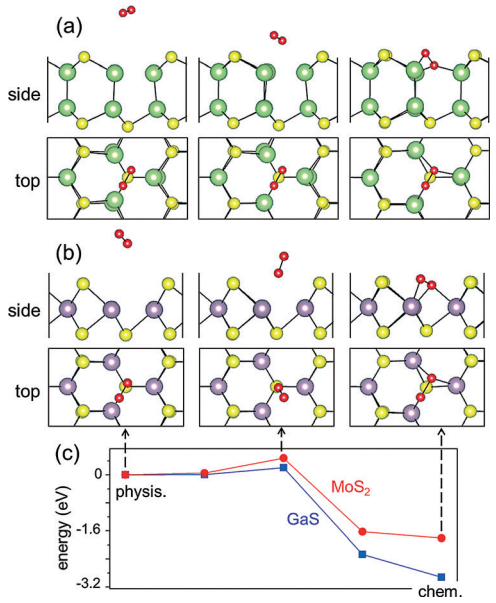

Figure 2. Reaction pathway of O_2 with V_X in a) GaS and b) MoS_2, from the physisorbed to chemisorbed state. S yellow, Ga green, Mo purple, O red. c) Energy evolution during the reaction, calculated by using PBE. See Figure 4 for a complete set of calculated barriers.

Although physisorbed molecules can modify the electronic structure of the defects by depleting/accumulating the charge densities,[3a,b,f,11] this modification is not stable at room temperature because the molecules can easily desorb or diffuse away from the defect sites. In contrast, the chemisorbed O_2 cannot be released at ambient conditions owing to the strongly exothermic adsorption; therefore, it can irreversibly change the properties of the defects. However, the chemisorption of O_2 does not occur spontaneously. As shown in Figure 2, a barrier must be overcome before reaching the chemisorbed state from the physisorbed state. The calculated barrier heights depend on the computational methods (see Figure 4); however, it is generally believed that PBE underestimates the barriers and the best estimate is given by the HSE functional.[12] We find from HSE calculations that MoS_2 has a larger barrier (0.74 eV) than that of GaS (0.48 eV). The reason why EX has a relatively small barrier will be explained later (see Figure 4 and the related text). According to the rate theory, the transition time from the physisorbed state to chemisorbed state is:

$$t \approx 1/(f\, e^{-E_b/k_b T}) \quad (2)$$

where f is attempt frequency, E_b is the barrier, k_b is the Boltzmann constant, and T is temperature. The f can be estimated by the flux of O_2 arriving at the V_X:

$$f \approx n\, v\, s_d \quad (3)$$

where n is O_2 density in air, v is the speed of the O_2 molecule, and s_d is the cross section of V_X, which can be taken as the square of lattice parameter. At room temperature and one atmospheric pressure, f is about 10^8 molecules s^{-1}, which gives $t \approx 20$ h for MoS_2 and 2 s for GaS.

Chemisorbed O_2 has a significant impact on the electronic structure of V_X. As shown in Figure 3, an intact V_X creates both deep acceptor and donor levels in GaS, and a deep acceptor level in MoS_2. These levels can trap the electrons or holes and scatter other charge carriers in the SC, thus reducing the carrier mobility. They can also non-radiatively recombine electrons and holes, resulting in a decrease of the quantum efficiency. Hence, V_X are typically harmful to the performance of the material (note that this is different from 2D black phosphorous, the intrinsic defects of which are relatively electronically benign[13]). However, upon O_2 chemisorption, the deep gap states are removed completely (Figure 3), converting V_X to electronically inactive sites. The elimination of the defect states is due to the isovalence

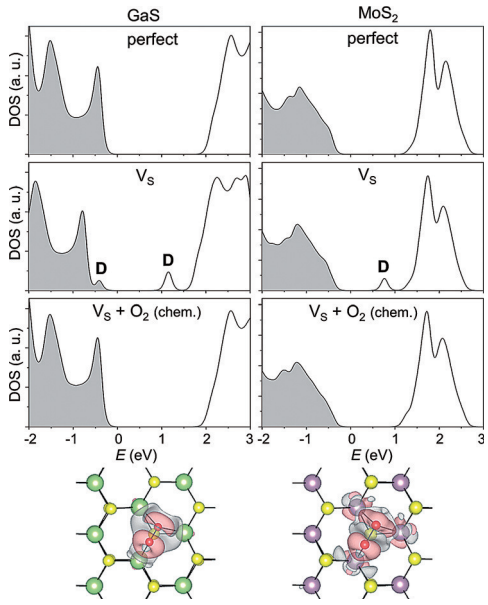

Figure 3. Density of states (DOS) for perfect GaS (left) and MoS_2 (right), and those containing V_X, and O_2 chemisorbed at the V_X site. The defect states are marked by "D" labels. Bottom: isosurface plots of the change of electron density after O_2 chemisorption, suggesting that electrons are transferred from V_X to the π^* orbitals of O_2. Gray: electron depletion; Pink: electron accumulation.

between the O_2 and X atom in 2D SCs. O_2 molecule has two singly occupied π^* orbitals (two unpaired electrons), which can obtain two electrons and make O_2 act as an element with the valence of −2, similar to that of the X atom in EX and MX_2. Therefore, O_2 chemisorption at V_X is equivalent to isovalent substitution of X by O_2; thus, the electronic structure of the SCs remains largely intact. As confirmation, Figure 3 (inset) shows the change of electron density after O_2 chemisorption. The electron density difference is defined as:

$$\Delta\rho = \rho(V_X + O_2) - \rho(V_X) - \rho(O_2) \quad (4)$$

where $\rho(V_X + O_2)$ is the electron density of the system with O_2 adsorbed on V_X site, $\rho(V_X)$ and $\rho(O_2)$ are the electron densities for isolated systems. We observe that electrons accumulate at O_2 by depleting those previously in V_X. The electron-accumulating region has a shape similar to that of π^*, indicating that π^* orbitals are now fully occupied and the dangling electrons in O_2 are paired up. This is further confirmed by the change of spin from triplet in isolated O_2 to singlet after chemisorption. As a result, the system becomes isovalent with that of the perfect SC, and thus, defect states are eliminated. This effect is generally applicable to other MX_2 and EX.

Figure 4 shows the trends of the chemisorption barriers across various commonly studied 2D SCs, calculated by using different methods. Note that some of the MX_2 or EX are not

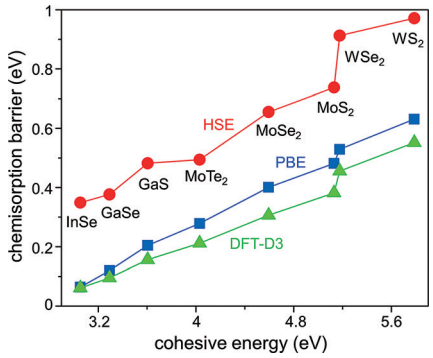

Figure 4. Trends of the O_2 chemisorption barriers at V_X for various 2D semiconductors, calculated by using different methods (HSE, PBE, and DFT-D3).

semiconductors (for example, WTe_2[14]), or do not exist in 2D (for example, InS), and therefore, they are excluded here. We observe that adding vdW corrections decreases the barriers, which is due to the enhancement of O_2 binding with the substrate. HSE always gives the highest values, which are closest to reality.[12] Regardless of the calculation methods, we find that the barriers decrease as the cohesive energy of the SC decreases. This is because the cohesive energy represents the stability of the material; thus, a less "stable" SC has a stronger tendency to chemisorb O_2 at V_X. For the same cations, the barriers drop from S to Se to Te; and for the same anions, the barriers increase from Ga to Mo to W. Consequently, WS_2 has the largest barrier of 0.97 eV, and therefore the O_2 chemisoprtion is kinetically forbidden at room temperature.

Chemisorbed O_2 at V_X can further dissociate into separated O atoms: one at the V_X site, and the other bound with the neighboring X to form an O–X group (Supporting Information, Figure S1). This dissociation also encounters barriers that depend on specific materials (Figure S1). However, compared with intact V_X, there are still no deep gap states (Supporting Information, Figure S2). This is because both O and the O–X group are isovalent with X atoms in these 2D SCs; therefore, the defect states due to the missing X is eliminated, as explained previously for chemisorbed O_2.

Our results suggest that it is possible to improve the transport properties and the quantum efficiency of the 2D chalcogenide SCs by O_2 treatment. An increase of temperature could help the reaction of O_2 with V_X in WS_2 and WSe_2, which have the highest barriers. However, the physisorbed O_2 at other sites of the basal plane can cause the nonuniform variation of the potential, leading to a scattering of the charge carriers.[3c,15] Therefore, it is important to remove these molecules after treatment; otherwise, they will compensate the improvement of the defect properties.

We note that several recent experimental studies show that the photoluminescence intensity of MX_2 is enhanced after air/O treatment.[3b,16] One possible mechanism that has been offered[3b,16] is the charge transfer between the environmental molecules and the V_X. Here we propose that these may partially result from the increase of quantum efficiency because of the suppressed non-radiative recombination at the V_X, thanks to the elimination of trap states by O_2/O. However, since the physisorbed O_2 (or other molecules) at other sites of the basal plane can also modify the optical properties of the MX_2 and contribute to the total photoluminescence variation, making a confirmative conclusion is too early at this stage. Nevertheless, it is encouraging to decouple these two contributions experimentally.

Although we focus on the 2D chalcogenide SCs herein, we believe that O_2 could also passivate the O vacancies in 2D oxide SCs, or perhaps other vacancies that have the missing atoms isovalent with O_2. In fact, the improved performance after air/O treatment has been observed in ZnO thin-film devices.[17]

In summary, by using the chalcogen vacancies as an example, we investigate the interaction between air and the defects in 2D SCs. O_2 is found to have the strongest impact that can change the vacancies from harmful carrier-traps to electronically benign sites. The electronic origin of this impact is explained and an effective way to improve the performance of 2D SCs is proposed.

Acknowledgements

This research was funded by the U.S. Department of Energy (DOE) under Contract No. DE-AC36-08GO28308. Y.L. and P.S. acknowledge support from DOE SETP DE-EE00025783 and DE-EE0006336. This work used the Peregrine supercomputer at National Renewable Energy Laboratory (NREL), as well as the computational resources at National

Energy Research Scientific Computing Center (NERSC), which is supported by the Office of Science of the DOE under Contract No. DE-AC02-05CH11231. Y.L. acknowledges computational resources and staff support from Lawrence Livermore National Laboratory (LLNL).

Keywords: chalcogens · computational chemistry · nanotechnology · oxygen · semiconductors

How to cite: *Angew. Chem. Int. Ed.* **2016**, *55*, 965–968
Angew. Chem. **2016**, *128*, 977–980

[1] a) G. Fiori, F. Bonaccorso, G. Iannaccone, T. Palacios, D. Neumaier, A. Seabaugh, S. K. Banerjee, L. Colombo, *Nat. Nanotechnol.* **2014**, *9*, 768–779; b) Q. H. Wang, K. Kalantar-Zadeh, A. Kis, J. N. Coleman, M. S. Strano, *Nat. Nanotechnol.* **2012**, *7*, 699–712; c) D. Akinwande, N. Petrone, J. Hone, *Nat. Commun.* **2014**, *5*, 5678; d) C. N. R. Rao, H. S. S. Ramakrishna Matte, U. Maitra, *Angew. Chem. Int. Ed.* **2013**, *52*, 13162–13185; *Angew. Chem.* **2013**, *125*, 13400–13424; e) Y. Hou, A. B. Laursen, J. Zhang, G. Zhang, Y. Zhu, X. Wang, S. Dahl, I. Chorkendorff, *Angew. Chem. Int. Ed.* **2013**, *52*, 3621–3625; *Angew. Chem.* **2013**, *125*, 3709–3713.

[2] X. Zou, B. I. Yakobson, *Acc. Chem. Res.* **2015**, *48*, 73–80.

[3] a) S. Tongay, J. Suh, C. Ataca, W. Fan, A. Luce, J. S. Kang, J. Liu, C. Ko, R. Raghunathanan, J. Zhou, F. Ogletree, J. Li, J. C. Grossman, J. Wu, *Sci. Rep.* **2013**, *3*, 2657; b) S. Tongay, J. Zhou, C. Ataca, J. Liu, J. S. Kang, T. S. Matthews, L. You, J. Li, J. C. Grossman, J. Wu, *Nano Lett.* **2013**, *13*, 2831–2836; c) H. Qiu, L. Pan, Z. Yao, J. Li, Y. Shi, X. Wang, *Appl. Phys. Lett.* **2012**, *100*, 123104; d) H.-Y. Park, M.-H. Lim, J. Jeon, G. Yoo, D.-H. Kang, S. K. Jang, M. H. Jeon, Y. Lee, J. H. Cho, G. Y. Yeom, W.-S. Jung, J. Lee, S. Park, S. Lee, J.-H. Park, *ACS Nano* **2015**, *9*, 2368–2376; e) D. J. Late, B. Liu, H. S. S. R. Matte, V. P. Dravid, C. N. R. Rao, *ACS Nano* **2012**, *6*, 5635–5641; f) B. Chen, H. Sahin, A. Suslu, L. Ding, M. I. Bertoni, F. M. Peeters, S. Tongay, *ACS Nano* **2015**, *9*, 5326–5332; g) J. O. Varghese, P. Agbo, A. M. Sutherland, V. W. Brar, G. R. Rossman, H. B. Gray, J. R. Heath, *Adv. Mater.* **2015**, *27*, 2734–2740; h) D. Kiriya, M. Tosun, P. Zhao, J. S. Kang, A. Javey, *J. Am. Chem. Soc.* **2014**, *136*, 7853–7856; i) S. S. Chou, Y.-K. Huang, J. Kim, B. Kaehr, B. M. Foley, P. Lu, C. Dykstra, P. E. Hopkins, C. J. Brinker, J. Huang, V. P. Dravid, *J. Am. Chem. Soc.* **2015**, *137*, 1742–1745.

[4] a) J. Hong, Z. Hu, M. Probert, K. Li, D. Lv, X. Yang, L. Gu, N. Mao, Q. Feng, L. Xie, J. Zhang, D. Wu, Z. Zhang, C. Jin, W. Ji, X. Zhang, J. Yuan, Z. Zhang, *Nat. Commun.* **2015**, *6*, 6293; b) Z. Yu, Y. Pan, Y. Shen, Z. Wang, Z.-Y. Ong, T. Xu, R. Xin, L. Pan, B. Wang, L. Sun, J. Wang, G. Zhang, Y. W. Zhang, Y. Shi, X. Wang, *Nat. Commun.* **2014**, *5*, 5290.

[5] a) G. Kresse, J. Hafner, *Phys. Rev. B* **1993**, *47*, 558–561; b) G. Kresse, J. Furthmüller, *Phys. Rev. B* **1996**, *54*, 11169–11186.

[6] a) P. E. Blöchl, *Phys. Rev. B* **1994**, *50*, 17953–17979; b) G. Kresse, D. Joubert, *Phys. Rev. B* **1999**, *59*, 1758–1775.

[7] J. P. Perdew, K. Burke, M. Ernzerhof, *Phys. Rev. Lett.* **1996**, *77*, 3865–3868.

[8] J. Paier, M. Marsman, K. Hummer, G. Kresse, I. C. Gerber, J. G. Ángyán, *J. Chem. Phys.* **2006**, *124*, 154709.

[9] S. Grimme, J. Antony, S. Ehrlich, H. Krieg, *J. Chem. Phys.* **2010**, *132*, 154104.

[10] G. Henkelman, B. P. Uberuaga, H. Jónsson, *J. Chem. Phys.* **2000**, *113*, 9901–9904.

[11] a) S. Zhao, J. Xue, W. Kang, *Chem. Phys. Lett.* **2014**, *595–596*, 35–42; b) Q. Yue, Z. Shao, S. Chang, J. Li, *Nanoscale Res. Lett.* **2013**, *8*, 425.

[12] J. F. Binder, A. Pasquarello, *Phys. Rev. B* **2014**, *89*, 245306.

[13] Y. Liu, F. Xu, Z. Zhang, E. S. Penev, B. I. Yakobson, *Nano Lett.* **2014**, *14*, 6782–6786.

[14] a) M. N. Ali, J. Xiong, S. Flynn, J. Tao, Q. D. Gibson, L. M. Schoop, T. Liang, N. Haldolaarachchige, M. Hirschberger, N. P. Ong, R. J. Cava, *Nature* **2014**, *514*, 205–208; b) I. Pletikosić, M. N. Ali, A. V. Fedorov, R. J. Cava, T. Valla, *Phys. Rev. Lett.* **2014**, *113*, 216601.

[15] X. Cui, G.-H. Lee, Y. D. Kim, G. Arefe, P. Y. Huang, C.-H. Lee, D. A. Chenet, X. Zhang, L. Wang, F. Ye, F. Pizzocchero, B. S. Jessen, K. Watanabe, T. Taniguchi, D. A. Muller, T. Low, P. Kim, J. Hone, *Nat. Nanotechnol.* **2015**, *10*, 534–540.

[16] H. Nan, Z. Wang, W. Wang, Z. Liang, Y. Lu, Q. Chen, D. He, P. Tan, F. Miao, X. Wang, J. Wang, Z. Ni, *ACS Nano* **2014**, *8*, 5738–5745.

[17] a) D. C. Olson, S. E. Shaheen, R. T. Collins, D. S. Ginley, *J. Phys. Chem. C* **2007**, *111*, 16670–16678; b) L. C. Cheng, W. M. Lun, L. K. Chung, H. Shih-Hua, C. Y. Sheng, L. Gong-Ru, H. J. Jang, *J. Disp. Technol.* **2009**, *5*, 192–197.

Received: September 21, 2015
Published online: November 24, 2015

